Asian Journal of Chemistry; Vol. 33, No. 11 (2021), 2626-2632

ASIAN JOURNAL OF CHEMISTRY

https://doi.org/10.14233/ajchem.2021.23349

Corrosion Inhibition of Mild Steel in 1 M HCl Solution by Poly(*o*-aminothiophenol) and Poly(*o*-aminothiophenol)/CuO Nanocomposites

U. Anto Maria Jeraldin and R. Jaya Santhi*

PG & Research Department of Chemistry, Auxilium College, Vellore-632006, India

*Corresponding author: E-mail: shanthijaya02@gmail.com

Received: 31 May 2021; *Accepted*: 20 July 2021; *Published online*: 20 October 2021; AJC-20540

The chemical oxidative polymerization of poly(*o*-aminothiophenol) and poly(*o*-aminothiophenol)/CuO nanocomposites were performed in aqueous HCl using ammonium persulfate as an oxidant. The synthesized polymer and its CuO nanocomposites were characterized by employing FT-IR, UV-Vis and XRD analysis. Weight loss and electrochemical techniques were used to investigate the inhibitory performance of poly(*o*-aminothiophenol) and poly(*o*-aminothiophenol)/CuO nanocomposites on mild steel in 1 M HCl solution. The electrochemical impedance spectroscopic method showed a capacitive loop, revealing that the corrosion reaction is governed by the charge transfer mechanism. The inhibitors were of a mixed type, according to polarization measurements. The adsorption process was obeyed by the Langmuir isotherm. The Langmuir adsorption isotherm was also used to derive thermodynamic adsorption parameters.

Keywords: Aminothiophenol, Nanocomposites, Corrosion, Mild steel, Electrochemical studies, Adsorption.

INTRODUCTION

Corrosion that occurs by rupturing of metals is an unpleasant process to nature; therefore, serious efforts are taken to check this phenomenon. Commonly applied three approaches to reduce the corrosion are anodic protection, cathodic protection and protective coatings [1]. Inspite of having many methods to control the metal corrosion, the application of conducting polymers for the inhibition of corrosion is an area which is recently gaining increasing attention [2].

Generally, polypyrrole (PPy), polyaniline (PANI) and their derivatives have been broadly studied because of their easy preparation and stability. The ring-substituted conducting polymers [3] like poly(*o*-toluidine), poly(*o*-anisidine), poly(*o*-chloroaniline) and poly(*m*-toluidine), can improve their anticorrosion performance in aggressive environment than the straight line polymers like PANI and PPy [4-7].

Aminothiophenols (ATP) are interesting electrochemical materials since both amine and thiol have different reactivities and thus provide more reactive sites. The productive use of this molecular assembly can give rise to remarkable morphologies, which leads to multiple applications. Poly(aminothiophenol) (PATP) is considered as one among the most interested conducting polymers and also attracted much interest in many studies with various practical applications because of its high conductivity, outstanding air stability and special physical, chemical properties differentiated with other conducting polymers [8-11]. Conducting polymers/inorganic metal oxide nanocomposites attracted considerable attention because of their physicochemical, electro-optical properties, unique microstructure and their effective usage in sensors, microelectronics and also in constructing nanoscopic assemblies and battery cathodes [12,13]. In the advancement of research in nanoscience, CuO nanoparticles have found multiple applications in various fields [14-17].

In view of these favourable characteristic properties, poly(*o*-aminothiophenol) (PoATP) and poly(*o*-aminothiophenol)/CuO (PoATP/CuO) nanocomposites have chosen for the synthesis and corrosion studies. To our best of knowledge, no reports in literature dealing with the anticorrosion properties of poly(*o*-aminothiophenol) and poly(*o*-aminothiophenol)/CuO nanocomposites on active metals. The main objective herein is to investigate the corrosion process of mild steel in 1 M HCl solution in the absence and presence of different concentrations of PoATP and PoATP/CuO and also to study the adsorption isotherm and mechanism.

EXPERIMENTAL

Monomer *o*-aminothiophenol (Alfa aezar), ammonium persulfate (Sigma-Aldrich) and hydrochloric acid were purchased from Merck Ltd., India. The CuO nanoparticle was purchased from Sigma-Aldrich. All the chemicals and reagents were of Analytical Grade and used as received without any further purification.

Synthesis of poly(*o*-aminothiophenol)/CuO nanocomposites: *o*-Aminothiophenol (monomer), ammonium persulfate (oxidant) and CuO were taken in 1:2:1 ratio. The monomer dissolved in 1 M HCl. The CuO nanoparticles were added to this solution with vigorous stirring to get a suspension. The oxidizing agent solution was slowly added into monomer and metal nanoparticle solution. The resultant solution was kept stirring for 5 h at 298 K, after that the brownish black powder obtained as residue. The polymer nanocomposites synthesized was washed with distilled water upto the filtrate became colourless then remove excess monomer, initiator and oligomers by using acetone and methanol. Finally, the resultant precipitate dried at 298 K for 24 h [18]. Same procedure was adopted for the synthesis of polymer.

Characterization: The FT-IR spectra of the synthesized polymer and its CuO nanocomposite were performed using Perkin-Elmer 1750 FTIR spectrophotometer at room temperature. UV-Vis spectra were recorded from 200-800 nm using Shimadzu model UV-2450 spectrophotometer by dissolving the polymer and its CuO nanocomposites in DMSO solvent. X-ray diffraction (XRD) was recorded with Bruker AXS D8 Advance diffractometer at room temperature ranging from 0º to 80º.

Electrochemical measurements: The anticorrosion activities of PoATP and PoATP/CuO at different concentrations ranging from 100 ppm to 750 ppm on pure mild steel in 1 M HCl were carried out by electrochemical techniques like potentiodynamic polarization method (PDP) and electrochemical impedance spectroscopy (EIS) using CHI 660E Electrochemical work station. An electrochemical cell with a three-electrode was used for electrochemical measurements; mild steel (area of 1 cm^2), a platinum electrode and a Ag/AgCl electrode (in 1M KCl) were used as working, counter and reference electrodes, respectively. The mild steel specimens were polished with a series of emery papers, followed by thorough rinsing in acetone and double distilled water and dried in air. Prior to any experiment, the substrates were treated as described and freshly used.

Potentiodynamic polarization method: The potentiodynamic current-potential curves were recorded by changing the electrode potential from open circuit potential (OCP) at a scan rate of 0.01 V/s. The corrosion inhibition efficiency (%IE) was evaluated for PoATP and PoATP/CuO at different concentrations using the following relationship [19].

$$IE\ (\%) = \frac{I^{o}_{corr} - I_{corr}}{I^{o}_{corr}} \times 100$$

where I^{o}_{corr} and I_{corr} are the corrosion current densities in the absence and the presence of the inhibitor.

Electrochemical impedance spectroscopy: To find the impedance parameters, the measured impedance data were fitted to an electric equivalent circuit. Thus the impedance parameters like the charge transfer resistance (R_{ct}) and the double-layer capacitance (C_{dl}) were calculated from the difference in impedance at low and high frequencies. Finally, the inhibition efficiency of the PoATP and PoATP/CuO has been calculated from charge transfer resistance using eqn. 1 [20]:

$$IE\ (\%) = \frac{R_{ct} - R^{o}_{ct}}{R_{ct}} \times 100 \quad (1)$$

where R_{ct} and R°_{ct} are the charge transfer resistance with and without inhibitor. Before every experiment, the surface area of the mild steel electrode exposed to the solution containing 1 M HCl with and without various concentrations of inhibitors.

Weight loss method: Corrosive medium 1 M HCl was prepared with double distilled water and the inhibitor solutions of PoATP and PoATP/CuO with different concentrations were employed in 1 M HCl. Specimen samples of mild steel coupon each having a surface area of 1 cm^2 were abraded with emery paper and washed with acetone then with distilled water and dried. The coupons were immersed into the aggressive solution for 2 h. The percentage of inhibition efficiency (%IE) of PoATP and PoATP/CuO were calculated using eqn. 2 [21].

$$IE\ (\%) = \frac{W^{o}_{corr} - W_{corr}}{W^{o}_{corr}} \times 100 \quad (2)$$

where W°_{corr} is the weight loss without inhibitor and W_{corr} is the weight loss with inhibitor.

Adsorption isotherm: Basic information on the interaction between an inhibitor and the metal surface was obtained by adsorption isotherm. The surface coverage (θ) of different concentrations of PoATP and PoATP/CuO can be related to using eqn. 3 [22]:

$$\theta = \frac{\%IE}{100} \quad (3)$$

The values of θ were used to find the best fitting adsorption model. The thermodynamic parameters like Gibb's free energy (ΔG_{ads}), equilibrium constant (K_{ads}) of the adsorption process were derived by using eqns. 4-6 [23,24]:

Langmuir isotherm:

$$\frac{C}{\theta} = C + \frac{1}{K_{ads}} \quad (4)$$

Freundlich isotherm:

$$\theta = K_{ads}\ C \quad (5)$$

$$\Delta G_{ads} = -RT\ \ln\ (55.5\ K_{ads}) \quad (6)$$

where C is the inhibitor concentration and R is the universal gas constant, T is the absolute temperature in K and the numerical value 55.5 is the molar concentration of water in acid solution.

RESULTS AND DISCUSSION

The FTIR spectra of PoATP and PoATP/CuO are illustrated in Fig. 1a. The bands at 1471 and 1620 cm^{-1} are assigned to C=C stretching vibrations of the quinonoid and benzenoid

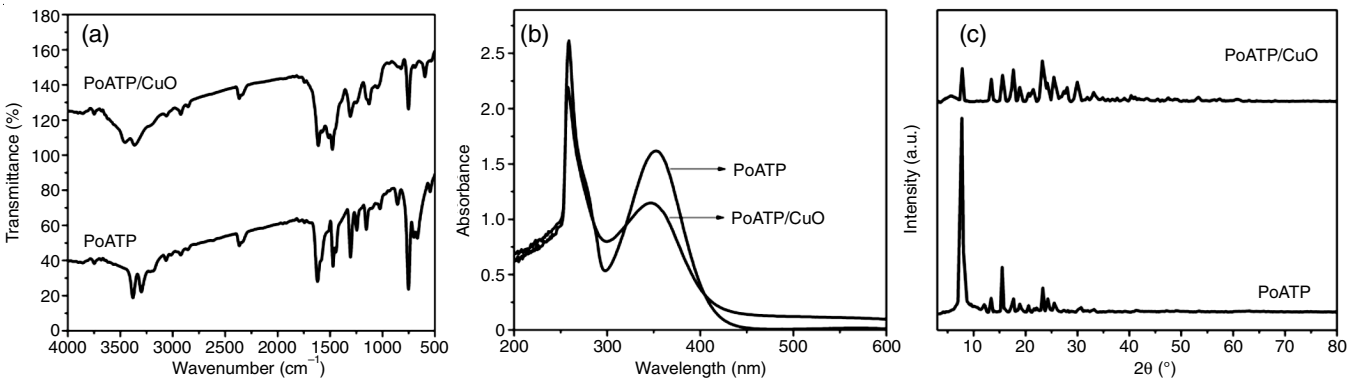

Fig. 1. (a) IR spectra (b) UV-Vis spectra and (c) XRD patterns of PoATP and PoATP/CuO

rings, which confirmed the formation of polymer [25]. The peaks at 3379 and 3300 cm^{-1} are associated with ν_{as}(N-H) and ν_s(N-H) stretching vibrations, respectively. The peak appears around 2360 cm^{-1} is the characteristics peak of S-H stretching [26]. The strong peak at 1101 cm^{-1} is considered to be stemmed from delocalization of electrons in polymeric backbone [27]. All the above peaks confirmed the polymerization of *o*-aminothiophenol. The PoATP/CuO has all the peaks of polymer but the values are slightly shifted towards higher wavenumber. The shift in the peaks of polymer nanocomposite is due to the formation of hydrogen bonding between CuO and NH group on the surface of PoATP and this can be explained on the basis of constrained growth of CuO in the presence of PoATP [28,29].

UV-Vis studies: Fig. 1b shows the UV-Vis spectra of poly-(*o*-aminothiophenol) and its CuO nanocomposites consist of two major absorption peaks. The peak at 259 nm for the polymer is assigned to π-π* transition of benzenoid rings. The second absorption peak at 352 nm is assigned to n-π* transition of the quinonoid ring [30]. The observation of hypsochromic shift in PoATP/CuO is because of the incorporation of metal oxide into the polymeric matrix [31] and it is also evident from Fig. 1b.

XRD studies: The XRD spectra of PoATP and PoATP/CuO are given in Fig. 1c. The diffraction patterns are typical of semi crystalline nature. The strong peaks exhibited by the polymer are characteristics 2θ values of the van der Waals distance between stacks of phenylene rings in PoATP [32]. The *d*-spacing [33] of highest intense crystalline peak in PoATP is found to be 3.4 Å. The degree of crystalline ordered structural pattern in PoATP owed to the more intrachain hydrogen bonding or electrostatic interaction through amine and thiol groups present in the polymer [34]. It can be seen from Fig. 1c, the intense diffractive peaks of PoATP has become weak in PoATP/CuO and it is because of the existence of the polymer layer on the surface of the nanoparticles, the molecular chain of PoATP is confined and the degree of crystallinity is decreased [35,36].

Anticorrosion studies of PoATP and PoATP/CuO

Potentiodynamic polarization: Polarization study was performed to collect the information about the cathodic and anodic kinetic reactions of the corrosion process [37]. Fig. 2 shows the Tafel curves for the mild steel in blank solution and at various concentrations of PoATP and PoATP/CuO at 298 K. The corrosion current density (I_{corr}) and corrosion potential (E_{corr}) were calculated by extrapolating the linear part of cathodic and anodic curves. The polarization parameters like E_{corr}, I_{corr}, surface coverage (θ) and inhibition efficiency (IE%) are listed in Table-1.

TABLE-1
COMPARISON OF PDP PARAMETERS
OF PoATP AND PoATP/CuO

Conc. (ppm)	E_{corr} (mV)	I_{corr} (μA/cm^2)	IE (%)	θ
Blank	-364	125.1	–	–
PoATP				
100	-358	40.9	67.30	0.67
250	-333	26.7	78.65	0.79
500	-289	22.9	81.69	0.81
750	-301	32.0	74.40	0.74
PoATP/CuO				
100	-324	37.80	69.78	0.70
250	-321	29.78	76.19	0.76
500	-312	13.23	89.42	0.89
750	-313	24.89	80.10	0.80

Absolute dissolution of mild steel in acid can be distinguished into cathodic, anodic half reactions [38-40] and the anodic reactions given below:

$$Fe + Cl^- \rightleftharpoons FeCl^-_{(ads)}$$

$$FeCl^-_{(ads)} \rightleftharpoons FeCl_{(ads)} + e^-$$

$$FeCl_{(ads)} \rightleftharpoons FeCl^+_{(ads)} + e^-$$

$$FeCl^+_{(ads)} \rightleftharpoons Fe^{2+} + Cl^-$$

whereas, cathodic reaction involves through the following steps [38-40]:

$$Fe + H^+ \rightleftharpoons FeH^+_{(ads)}$$

$$FeH^+_{(ads)} + e^- \rightleftharpoons FeH_{(ads)}$$

$$FeH_{(ads)} + H^+ + e^- \rightleftharpoons Fe + H_2$$

Fig. 2 clearly shows that in case of inhibited solution both anodic and cathodic region of the Tafel curves shift towards the lower corrosion current density, which may be due to the development of protective film by PoATP and PoATP/CuO

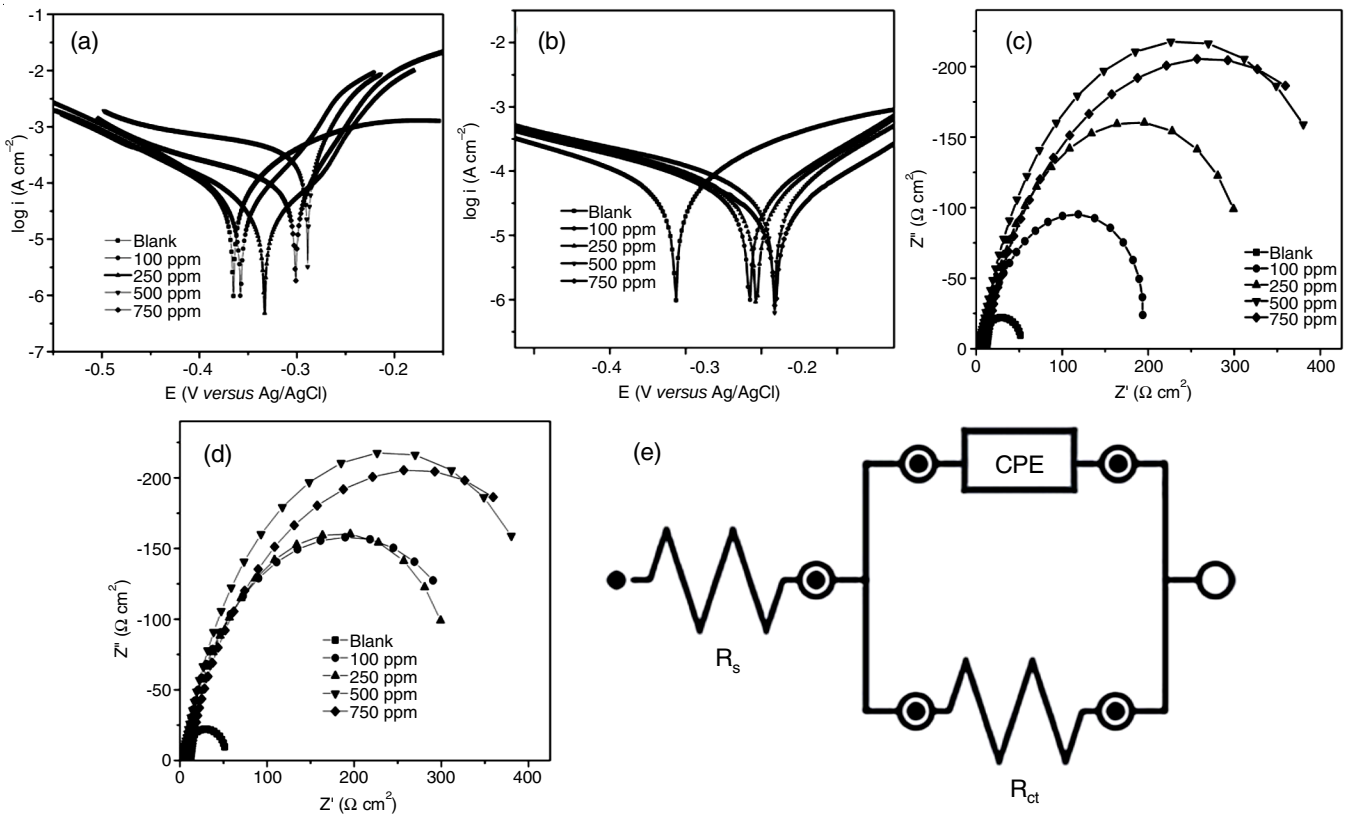

Fig. 2. Tafel plots of (a) PoATP and (b) PoATP/CuO and Nyquist plots of (c) PoATP, (d) PoATP/CuO and (e) equivalent circuit of Nyquist curves

on the metal surface [41]. Moreover, the addition of PoATP and PoATP/CuO do not alter the value of E_{corr} significantly (change is less than 85 mV), which indicate the mixed type inhibitors [42].

From Table-1, it is evident that the corrosion current density (I_{corr}) values were found to decrease with increase in concentrations for the PoATP and PoATP/CuO, respectively, which confirmed the adsorption of inhibitors on the metal surface and hence inhibition occurs and this decrease in the I_{corr} value is more pronounced at higher concentrations of PoATP and PoATP/CuO. As the concentrations increase from 100 to 500 ppm, the % IE increases up to 81.6% for PoATP and 89.4% for PoATP/CuO. Further increase in the concentration to 750 ppm leads to decrease in the inhibition efficiency, which shows that 500 ppm is the optimum concentration for both PoATP and PoATP/CuO.

Electrochemical impedance spectroscopy: The anti-corrosion activities of PoATP and PoATP/CuO at various concentrations were analyzed by EIS technique. The Nyquist plots are given in Fig. 2c-d with an equivalent circuit Fig. 2e as well as the EIS parameters are given in Table-2. Here, CPE was used at the place of pure double layer capacitance (C_{dl}) to consider the effect of roughness and heterogeneities on the mild steel surface and grain boundaries [43,44].

It is clear from Fig. 2c-d that Nyquist plots for mild steel in blank also in inhibited solution has similar appearance which means that polymer and nanocomposites are reducing corrosion without changing its mechanism [45]. The Nyquist plots consist

TABLE-2
COMPARISON OF EIS PARAMETERS OF PoATP AND PoATP/CuO

Conc. (ppm)	C_{dl} (μF/cm^2)	R_{ct} (Ω cm^2)	IE (%)	θ
Blank	102.2	36.43	–	–
PoATP				
100	94.8	107.3	66.05	0.66
250	75.3	194.8	81.30	0.81
500	19.2	398.1	90.84	0.91
750	22.7	253.3	85.62	0.86
PoATP/CuO				
100	89.3	101.3	64.04	0.64
250	61.5	183	80.09	0.80
500	20.6	637	94.28	0.94
750	31.4	298	87.80	0.88

of depressed semicircles with centers under the real axis, which are because of frequency dispersion of interfacial impedance. This phenomenon can be usually attributed to different factors like adsorption of inhibitors, inhomogeneity of electrode surface and impurities [46].

The %IE were found to be 0%, 66%, 81%, 90.8% and 85.6% for blank, 100 ppm, 250 ppm, 500 ppm and 750 ppm for PoATP. The highest IE 94%, for chemically synthesized CuO embedded PoATP, was observed at the concentration of 500 ppm, respectively. Table-2 shows that that the increase in inhibitors concentration from 100 to 500 ppm increases the %IE of mild steel in 1 M HCl at 298 K. Further increasing the concentration of PoATP and PoATP/CuO to 750 ppm shows a

sudden decrease in %IE and the EIS parameters start to follow the opposite trend [47] and reveals that the optimum concentration of inhibitors is 500 ppm. The results showed that increasing the concentration of PoATP and PoATP/CuO, leads to a substantial increase in R_{ct} values suggesting that inhibitors retard the charge transfer reaction rate by getting adsorbed over mild steel surface and thus inhibiting rate of corrosion [48].

Table-2 shows that the value of C_{dl} with inhibitors is less than C_{dl} value in case of blank. The decline in C_{dl} values may be because of the reduction in local dielectric constant and rise in the electrical double layer thickness. This increase in thick-ness of electric double layer is due to adsorption of PoATP and PoATP/CuO over the mild steel surface. This finding also supports that the inhibition of mild steel corrosion owed to the adsorption mechanism [49].

Weight loss method measurements: The %IE by weight loss method for polymer PoATP and PoATP/CuO nanocomposites on mild steel in 1 M HCl at various concentrations were studied after 2 h of immersion of mild steel at 298 K.

Variation of inhibition efficiency with the concentration of PoATP and PoATP/CuO is observed and corrosion parameters like surface coverage (θ) and inhibition efficiency (% IE) are reported in Table-3. It is clear from the results that the %IE of PoATP, PoATP/CuO increases and reaches to a maximum value at optimum concentration (500 ppm). The higher inhibition at the optimum concentration may be due to the increase in surface coverage by reason of adsorption of PoATP and PoATP/CuO on the mild steel surface thus blocking the active sites and isolating the mild steel surface from corrosive environment [50]. The results attained from weight loss method were in good agreement with in PDP and EIS results.

TABLE-3
THE WEIGHT LOSS PARAMETERS OF PoATP AND PoATP/CuO

Inhibitor	Conc. (ppm)	θ	IE (%)
PoATP	100	0.56	56.34
	250	0.67	66.91
	500	0.78	78.09
	750	0.71	71.23
PoATP/CuO	100	0.68	67.89
	250	0.76	75.84
	500	0.85	84.77
	750	0.80	79.63

Adsorption isotherm and thermodynamic parameters: The interaction between the PoATP and PoATP/CuO with mild steel surface can be provided by the adsorption isotherm. So the study of adsorption isotherm becomes very crucial to understand the mechanism of inhibition. To study the isotherm, the linear relation between surface coverage (θ) values and inhibitor concentration (C_{inh}) is needed. Attempts were made to fit the θ values to Langmuir and Freundlich isotherms. By far the best fit was obtained with the Langmuir isotherm for both PoATP and PoATP/CuO systems [51,52].

The plot of Langmuir isotherm in Fig. 3a gives a straight line between C_{inh} and (C_{inh}/θ) with regression coefficient R^2 values, which are very close to unity. The strong correlations ($R^2 = 0.990$ for PoATP, $R^2 = 0.996$ for PoATP/CuO) confirmed

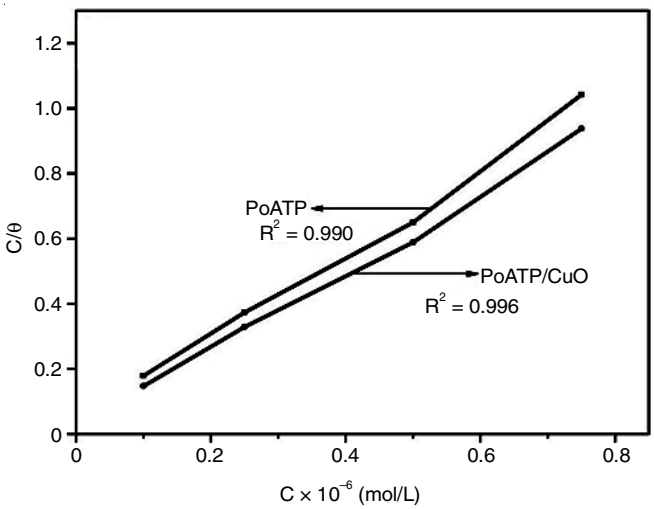

Fig. 3a. Langmuir isotherm plot of PoATP and PoATP/CuO

the validity of this approach and K_{ads} values of PoATP and PoATP/CuO were calculated and reported as 31.25×10^3 L/mol and 76.92×10^3 L/mol, respectively. It is well established that value of K_{ads} represents the strength of adsorption of PoATP and PoATP/CuO on the mild steel surface.

The higher values of K_{ads} for studied polymer and its CuO nanocomposites indicate stronger adsorption on the mild steel surface in 1 M HCl solution and hence, which leads to higher inhibition efficiency [53]. This can be explained by the presence of hetero-atoms and π-electrons in the polymeric backbone. These data supported the good performance of PoATP and PoATP/CuO as corrosion inhibitors for mild steel in 1 M HCl. The proposed mode of adsorption of PoATP on mild steel in 1 M HCl is schematically represented in Fig. 3b.

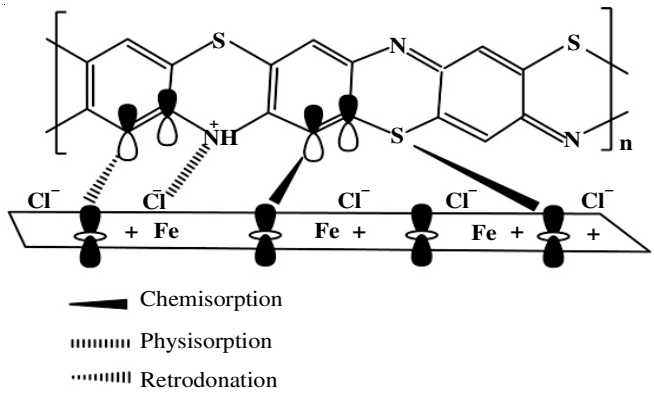

Fig. 3b. Adsorption mechanism of PoATP on mild steeel in 1 M HCl

The K_{ads} values are related with the standard free energy of adsorption (ΔG°_{ads}) and the calculated negative values of ΔG°_{ads}, were consistent with the adsorption process's spontaneity and adsorbed layer stability of the PoATP and PoATP/CuO on the mild steel surface. In present case, the calculated values of ΔG_{ads} for PoATP and PoATP/CuO were -35.59 KJ/mol and -37.82 KJ/mol. Since these values are between -20 and -40 KJ/mol, it can be concluded that PoATP and PoATP/CuO adsorb on MS *via* both physisorption [54,55] and chemisorption [56] but predominantly through chemisorption.

Conclusion

In this work, poly(*o*-aminothiophenol) and CuO nanoparticles embedded poly(*o*-aminothiophenol) were synthesized, characterized and utilized as effective corrosion inhibitors for mild steel in 1 M HCl. The inhibition efficiency increases with concentration and maximum efficiency was found at the optimum concentration of 500 ppm. The percentage of inhibition efficiency was greater for PoATP/CuO than the pure polymer PoATP. The order of inhibition efficiency studied by electrochemical impedance spectroscopy (EIS), potentiodynamic polarization (PDP) and weight loss method were in good agreement with each other and both polymers PoATP and PoATP/CuO nanocomposites behaved as efficient mixed type of corrosion inhibitors for mild steel in 1 M HCl. These polymer and nanocomposites inhibited corrosion by adsorption mechanism. The adsorption of PoATP and PoATP/CuO was spontaneous and followed Langmuir isotherm and the values of standard free energy showed that the adsorption of them on mild steel in 1 M HCl was predominantly through chemisorption.

CONFLICT OF INTEREST

The authors declare that there is no conflict of interests regarding the publication of this article.

REFERENCES

1. A. Olad and B. Naseri, *Prog. Org. Coat.*, **67**, 233 (2010); https://doi.org/10.1016/j.porgcoat.2009.12.003
2. R. Manickavasagam, K. Jeya Karthik, M. Paramasivam and S. Venkatakrishna Iyer, *Anti-Corros. Methods Mater.*, **49**, 19 (2002); https://doi.org/10.1108/00035590210413566
3. D. Sazou, *Synth. Met.*, **118**, 133 (2001); https://doi.org/10.1016/S0379-6779(00)00399-4
4. U. Rammelt, P.T. Nguyen and W. Plieth, *Electrochim. Acta*, **46**, 4251 (2001); https://doi.org/10.1016/S0013-4686(01)00688-0
5. S.S. Abd El Rehim, S.M. Sayyah, M.M. El-Deeb, S.M. Kamal and R.E. Azooz, *Mater. Chem. Phys.*, **123**, 20 (2010); https://doi.org/10.1016/j.matchemphys.2010.02.069
6. T. Tuken, G. Tansug, B. Yazici and M. Erbil, *Surf. Coat. Technol.*, **202**, 146 (2007); https://doi.org/10.1016/j.surfcoat.2007.05.022
7. V. Patil, S.R. Sainkar and P.P. Patil, *Synth. Met.*, **140**, 57 (2004); https://doi.org/10.1016/S0379-6779(02)01323-1
8. L.-J. Kong, M.-F. Pan, G.-Z. Fang, K. Qian and S. Wang, *Anal. Bioanal. Chem.*, **404**, 1653 (2012); https://doi.org/10.1007/s00216-012-6253-7
9. A. Uzer, S. Saglam, Z. Can, E. Erçag and R. Apak, *Int. J. Mol. Sci.*, **17**, 1253 (2016); https://doi.org/10.3390/ijms17081253
10. A.I. Gopalan, K.P. Lee, K.M. Manesh, P. Santhosh, J.H. Kim and J.S. Kang, *Talanta*, **71**, 1774 (2007); https://doi.org/10.1016/j.talanta.2006.08.026
11. J. Lukkari, K. Kleemola, M. Meretoja, T. Ollonqvist and J. Kankare, *Langmuir*, **14**, 1705 (1998); https://doi.org/10.1021/la970931x
12. R. Gangopadhyay and A. De, *Chem. Mater.*, **12**, 608 (2000); https://doi.org/10.1021/cm990537f
13. Y.C. Liu, J.M. Huang, C.E. Tsai, T.C. Chuang and C.-C Wang, *Chem. Phys. Lett.*, **387**, 155 (2004); https://doi.org/10.1016/j.cplett.2004.02.014
14. A. Mittiga, E. Salza, F. Sarto, M. Tucci and R. Vasanthi, *Appl. Phys. Lett.*, **88**, 163502 (2006); https://doi.org/10.1063/1.2194315
15. P. Somani, A.B. Mandale and S. Radhakrishnan, *Acta Mater.*, **48**, 2859 (2000); https://doi.org/10.1016/S1359-6454(00)00098-7
16. F.A. Bezza, S.M. Tichapondwa and E.M.N. Chirwa, *Sci. Rep.*, **10**, 16680 (2020); https://doi.org/10.1038/s41598-020-73497-z
17. M.R. Nabid, R. Sedghi, A. Bagheri, M. Behbahani, M. Taghizadeh, H.A. Oskooie and M.M. Heravi, *J. Hazard. Mater.*, **203-204**, 93 (2012); https://doi.org/10.1016/j.jhazmat.2011.11.096
18. K.D. Kim, S.S. Kim, Y-H. Choa and H.T. Kim, *J. Ind. Eng. Chem.*, **13**, 1137 (2007).
19. M.E. Mashuga, L.O. Olasunkanmi and E.E. Ebenso, *J. Mol. Struct.*, **1136**, 127 (2017); https://doi.org/10.1016/j.molstruc.2017.02.002
20. Y. Elkacimi, M. Achnin, Y. Aouine, M.E. Touhami, A. Alami, R. Touir, M. Sfaira, D. Chebabe, A. Elachqar and B. Hammouti, *Port. Electrochem. Acta*, **30**, 53 (2012); https://doi.org/10.4152/pea.201201053
21. L. Zhang, Y. He, Y. Zhou, R. Yang, Q. Yang, D. Qing and Q. Niu, *Petroleum*, **1**, 237 (2015); https://doi.org/10.1016/j.petlm.2015.10.007
22. N.A. Negm, M.F. Zaki, M.M. Said and S.M. Morsy, *Corros. Sci.*, **53**, 4233 (2011); https://doi.org/10.1016/j.corsci.2011.08.034
23. A. Kosari, M.H. Moayed, A. Davoodi, R. Parvizi, M. Momeni, H. Eshghi and H. Moradi, *Corros. Sci.*, **78**, 138 (2014); https://doi.org/10.1016/j.corsci.2013.09.009
24. W. Li, Q. He, S. Zhang, C. Pei and B. Hou, *J. Appl. Electrochem.*, **38**, 289 (2008); https://doi.org/10.1007/s10800-007-9437-7
25. M.R. Nabid, R. Sedghi, P.R. Jamaat, N. Safari and A.A. Entezami, *J. Appl. Catal. A.*, **328**, 52 (2007); https://doi.org/10.1016/j.apcata.2007.05.017
26. D. He, Y. Wu and B.Q. Xu, *Eur. Polym. J.*, **43**, 3703 (2007); https://doi.org/10.1016/j.eurpolymj.2007.06.038
27. M.R. Nabid, R. Sedghi, A.B. Moghaddam, M. Barari, P.R. Jamaat and N. Safari, *J. Porphyr. Phthalocyanines*, **13**, 980 (2009); https://doi.org/10.1142/S1088424609001248
28. T. Mathavan, J. Archana, Y. Hayakawa, K. Anitha, M.A. Jothirajan, A. Divya and A.M.F. Benial, *Int. J. Chemtech Res.*, **7**, 1253 (2015).
29. Q. Du, W. Zhang, H. Ma, J. Zheng, B. Zhou and Y. Li, *Tetrahedron*, **68**, 3577 (2012); https://doi.org/10.1016/j.tet.2012.03.008
30. S.K. Shukla, M.A. Quraishi and R. Prakash, *Corros. Sci.*, **50**, 2867 (2008); https://doi.org/10.1016/j.corsci.2008.07.025
31. M.V. Kulkarni, A.K. Viswanath and U.P. Malik, *Mater. Chem. Phys.*, **89**, 1 (2005); https://doi.org/10.1016/j.matchemphys.2004.01.031
32. C. Saravanan, S. Palaniappan and F. Chandezon, *Mater. Lett.*, **62**, 882 (2008); https://doi.org/10.1016/j.matlet.2007.07.003
33. S. Bhadra, N.K. Singha and D. Khastgir, *Eur. Polym. J.*, **44**, 1763 (2008); https://doi.org/10.1016/j.eurpolymj.2008.03.010
34. H. Xia and Q. Wang, *Chem. Mater.*, **14**, 2158 (2002); https://doi.org/10.1021/cm0109591
35. S. Islam, M. Ganaie, S. Ahmad, A.M. Siddiqui and M. Zulfequar, *Int. J. Phys. Astron.*, **2**, 105 (2014).
36. N.S. Alghunaim, *Results Phys.*, **5**, 331 (2015); https://doi.org/10.1016/j.rinp.2015.11.003
37. M. ElBelghiti, Y. Karzazi, A. Dafali, B. Hammouti, F. Bentiss, I.B. Obot, I. Bahadur and E.E. Ebenso, *J. Mol. Liq.*, **218**, 281 (2016); https://doi.org/10.1016/j.molliq.2016.01.076
38. X. Zhou, H. Yang and F. Wang, *Electrochim. Acta*, **56**, 4268 (2011); https://doi.org/10.1016/j.electacta.2011.01.081
39. M. Valcarce and M. Vázquez, *Electrochim. Acta*, **53**, 5007 (2008); https://doi.org/10.1016/j.electacta.2008.01.091
40. A. Yousefi, S. Javadian, N. Dalir, J. Kakemam and J. Akbari, *RSC Adv.*, **5**, 11697 (2015); https://doi.org/10.1039/C4RA10995C

41. N.K. Gupta, C. Verma, M.A. Quraishi and A.K. Mukherjee, *J. Mol. Liq.*, **215**, 47 (2016); https://doi.org/10.1016/j.molliq.2015.12.027
42. R.E. Morsi, E.A. Khamis and A.M. Al-Sabagh, *J. Taiwan Inst. Chem. Eng.*, **60**, 573 (2016); https://doi.org/10.1016/j.jtice.2015.10.028
43. C. Christodoulou, C.I. Goodier, S.A. Austin, J. Webb and G. Glass, *Corros. Sci.*, **62**, 176 (2012); https://doi.org/10.1016/j.corsci.2012.05.014
44. R. Álvarez-Bustamante, G. Negrón-Silva, M. Abreu-Quijano, H. Herrera-Hernández, M. Romero-Romo, A. Cuán and M. Palomar-Pardavé, *Electrochim. Acta*, **54**, 5393 (2009); https://doi.org/10.1016/j.electacta.2009.04.029
45. L.O. Olasunkanmi, I.B. Obot, M.M. Kabanda and E.E. Ebenso, *J. Phys. Chem. C*, **119**, 16004 (2015); https://doi.org/10.1021/acs.jpcc.5b03285
46. P. Singh, E.E. Ebenso, L.O. Olasunkanmi, I.B. Obot and M.A. Quraishi, *J. Phys. Chem. C*, **120**, 3408 (2016); https://doi.org/10.1021/acs.jpcc.5b11901
47. N. Soltani, N. Tavakkoli, M. Khayat Kashani, A. Mosavizadeh, E.E. Oguzie and M.R. Jalali, *J. Ind. Eng. Chem.*, **20**, 3217 (2014); https://doi.org/10.1016/j.jiec.2013.12.002
48. Z. Zhang, N.C. Tian, X.D. Huang, W. Shang and L. Wu, *RSC Adv.*, **6**, 22250 (2016); https://doi.org/10.1039/C5RA25359D
49. K.R. Ansari, M.A. Quraishi and A. Singh, *J. Ind. Eng. Chem.*, **25**, 89 (2015); https://doi.org/10.1016/j.jiec.2014.10.017
50. D.K. Singh, S. Kumar, G. Udayabhanu and R.P. John, *J. Mol. Liq.*, **216**, 738 (2016); https://doi.org/10.1016/j.molliq.2016.02.012
51. M. Kissi, M. Bouklah, B. Hammouti and M. Benkaddour, *Appl. Surf. Sci.*, **252**, 4190 (2006); https://doi.org/10.1016/j.apsusc.2005.06.035
52. E. Machnikova, K.H. Whitmire and N. Hackerman, *Electrochim. Acta*, **53**, 6024 (2008); https://doi.org/10.1016/j.electacta.2008.03.021
53. I.B. Obot and N.O. Obi-Egbedi, *Colloids Surf. A Physicochem. Eng. Asp.*, **330**, 207 (2008); https://doi.org/10.1016/j.colsurfa.2008.07.058
54. K. Zakaria, N.A. Negm, E.A. Khamis and E.A. Badr, *J. Taiwan Inst. Chem. Eng.*, **61**, 316 (2016); https://doi.org/10.1016/j.jtice.2015.12.021
55. I. Ahamad, R. Prasad and M.A. Quraishi, *Corros. Sci.*, **52**, 933 (2010); https://doi.org/10.1016/j.corsci.2009.11.016
56. N. Kicir, G. Tansug, M. Erbil and T. Tuken, *Corros. Sci.*, **105**, 88 (2016); https://doi.org/10.1016/j.corsci.2016.01.006